Drop/Shock Behavior of Low Temperature Solder BGA

Sufyan Tahat, Sa'd Hamasha, Ph.D.
Auburn University
Al, USA
Sat0063@auburn.edu

Michael Meilunas
Universal Instruments Corporation
NY, USA
meilunas@uic.com

ABSTRACT

As electronic devices continue to expand into all aspects of modern life, the demand for reliable soldering materials has become more critical. The transition to lead-free alternatives has led to the emergence of high-temperature Tin-Silver-Copper alloys and low-temperature Tin-Bismuth alloys, each adapted to specific applications. This study examines challenges posed by aging, a critical factor influencing the long-term performance of solder joints. Aging, often associated with gradual material changes, can impact mechanical and thermal properties, potentially compromising the reliability of electronic assemblies. To address these challenges, this research utilized controlled aging conditions to simulate real-world scenarios, with a particular focus on room temperature aging for two alloys: SAC305 and L29. Samples were evaluated using drop/shock testing to assess the durability of BGA solder joints under mechanical stress shortly after assembly and up to 50 days later when stored at room temperature. Results showed that aging at room temperature enhanced the reliability of L29 alloy but had negligible impact on the SAC305 alloy.

Key words: LTS, aging, reliability, drop testing, SAC305

INTRODUCTION

In recent years, the continuous integration of electronics into all aspects of daily life has required further development of robust and reliable soldering materials [1]. These requirements hold especially true for portable products like laptop computers and smartphones, which have specific mechanical reliability needs [2]. As the market for portable electronics continues to grow rapidly, the increasing complexity of these devices introduces novel challenges. Traditionally, eutectic SnPb solder alloys had been the norm in electronic assemblies. However, the European Union's RoHS directive has steered the industry towards lead-free alternatives, driven by both environmental concerns and health considerations related to lead-containing solder alloys. This shift towards safer alternatives drove the emergence of Sn-Ag-Cu (SAC) solder alloys as replacements for lead-based alloys [2,3,4], but brought with it a need for higher reflow temperatures which now prove problematic in some instances.

Currently, three primary solder reflow categories based on peak processing temperatures are available for different manufacturing needs: high-temperature solders (>250°C Celsius), medium-temperature solders (200 - 220°C), and low-temperature solders (LTS; 130-200°C) [5]. SAC alloys, classified as high-temperature solders, are frequently used in scenarios where solder joints face challenging thermal and mechanical stresses, especially in sectors like automotive and avionics while low-temperature solder usage has been fueled by the desire for slimmer, lighter, and higher-performing consumer electronic products with less demanding thermo-mechanical requirements [5,6,7]. Additionally, low-temperature soldering may reduce manufacturing costs as energy expenditures directly related to the soldering process are lower than with SAC alloys [8].

Navigating the challenges posed by thinner package dimensions during reflow soldering assembly is a primary factor driving LTS integration. Thin packages have a propensity to warp at typical reflow temperatures and by reducing the peak reflow temperature, warpage-induced defects such as Head on Pillow (HoP) and Non-Wet can be reduced or eliminated.

Among the array of solder alloys, SAC305 and LTS alloys have gained substantial attention due to their versatile applications, mechanical resilience, and environmental sustainability [10]. It's crucial to highlight the significant influence of bismuth (Bi) on these solder alloys. Research indicates that Bi has the potential to lower the melting temperature, enhance tensile strength, and reduce elongation [1,10,11]. Furthermore, Bi contributes to improved wettability in SAC alloys [12]. Research studies revealed that small amounts of Bi demonstrate increased resistance to crack formation, owing to the strengthening effect of Bi. However, it's worth noting that exceeding a certain Bi concentration level can be detrimental to the mechanical properties [13].

The effects of aging on these alloys have emerged as critical considerations in the quest to ensure the long-term reliability of electronic assemblies. Room temperature aging, also referred to as ambient aging, simulates the exposure of solder joints to real-world conditions [14]. This process is marked by gradual material changes that can potentially affect the mechanical and thermal properties of solder alloys, consequently influencing their overall reliability. As a rule of thumb, materials with homologous temperatures above 0.5 are expected to evolve rapidly and LTS alloys with melting temperatures around 140°C have homologous temperatures of approximately 0.72 at room temperature which is significantly greater than the 0.61 homologous temperature of SAC305 at room temperature.

Investigating room temperature aging provides valuable insights into the long-term behavior of solder joints in electronic devices. Subjecting electronic components to isothermal preconditioning at room temperature can lead to a reduction in their lifespan [16]. Chuang et al. [15] conducted a study examining the influence of aging on microstructure at room temperature. Their research revealed that following a six-month period of aging at room temperature, key parameters such as ultimate strength, stiffness, strain, and yield stress experienced a notable decline of approximately 40%. Furthermore, Hani et al. [16] investigated the impact of varying aging temperatures and times on the shear strength of SAC305. Their study highlighted that the aging time had a significantly more pronounced effect on shear strength compared to aging temperature. Increasing the aging duration was found to substantially decrease shear strength. A similar trend was observed by Kim et al. [17], who noted a 5% reduction in solder material strength following 300 hours of aging at 150°C. Longer aging durations were found to correspond with decreased reliability, reduced inelastic work per cycle, and an increase in plastic strain. Ma et al. [18] utilized a set of assembled test boards that underwent preconditioning (thermal aging) at temperatures of 75°C, 100°C, and 150°C, with holding times of 500 and 1000 hours, prior to shock testing. These preconditioned boards, along with non-aged boards at room temperature, were subjected to mechanical shock tests. Their findings demonstrated that the non-aged assembled boards exhibited the highest shock resistance values, while aging was found to significantly deteriorate shock performance.

While these alloys hold promise, understanding their aging characteristics is pivotal to ensuring long-term reliability. Thus, the primary objective of this study is to assess room temperature aging impact on the reliability of LTS solder joints while using SAC solder for rough comparative purposes. By subjecting these alloys to controlled aging conditions, changes in mechanical properties, microstructure, and intermetallic compound formation will be observed. Subsequent drop testing will evaluate the ability of aged solder joints to endure mechanical stresses and maintain their integrity. Findings have the potential to inform material selection, manufacturing practices, and electronic assembly design; enhancing the long-term performance of electronic devices in an ever-evolving landscape.

MATERIALS AND METHOD

Test Sample Preparation:

The test vehicle includes a 6-layer printed circuit board (PCB) with a dummy 556 I/O Ball Grid Array (BGA) component soldered at its center. The test board measured 100x100mm and was 1mm thick. The board contained eight tooling holes, located in a circular pattern of 46.7mm radius from the center of the test board. The board was acquired with a copper Organic Solderability Preservative (OSP) surface finish. The test board attachment pads for BGA soldering were solder mask defined (SMD) with 0.38mm diameter openings. SMD pads were chosen for the experiment to ensure that the test samples failed due to some form of solder fatigue and/or fracture and not PCB pad cratering or other non-solder failure mechanisms that may occur during drop/shock testing.

The BGA component was designed with 1.0mm bump pitch and SMD pads with 0.38mm diameter mask openings. The BGA pads were Electroless Nickel Immersion Gold (ENIG) finished. The BGA was produced with SAC305 (96.5Sn-3Ag-0.5Cu) and low-temperature L29 (Sn/58Bi/Sb/Ni) solder alloys using 0.4mm diameter solder spheres.

When assembled, the BGA and PCB formed a single daisy-chained solder joint loop consisting of the 80 outermost solder joints which could then be electrically monitored during drop/shock testing. Multiple probe points were also provided on the test board which allowed for individual joints and blocks of joints to be electrically examined during and/or after drop testing in order to assist in failure isolation.

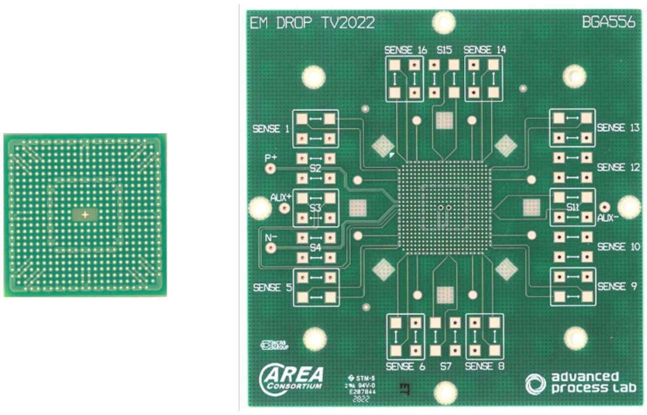

Figure 1. Component and test board

Two assembly processes were used to create the test vehicles. The SAC305 samples were assembled using a no-clean SAC305 solder paste and a convective oven reflow process in which the samples were heated to 243ºC with a time above liquidus (217°C) of 63 seconds as measured near the BGA solder joints. The L29 samples were assembled using a no-clean L29 solder paste and a convective oven reflow process in which the samples were heated 185°C with a time above liquidus (140°C) of 73seconds as measured near the BGA solder joints.

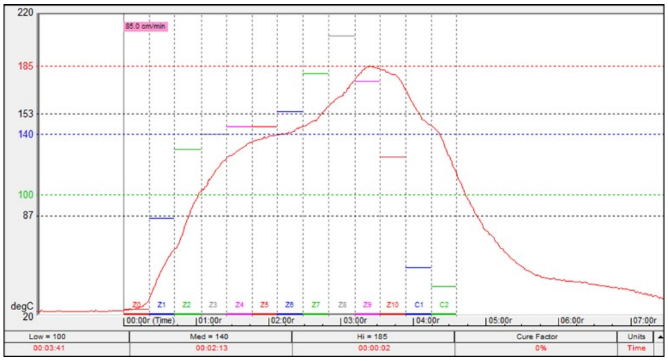

Figure 2. L29 Reflow Profile

Testing Method:

Drop/shock testing was used to assess the reliability of the solder joints. Figure 3 shows the drop table that was used for the experiment as well as the monitoring equipment. The test boards were mounted to the drop table with the BGA side facing downward using the four corner-most tooling holes to bolt the boards to 12mm hex standoffs. Input acceleration during each drop event was measured with an accelerometer that was mounted directly to the drop table.

Figure 2. Experimental setup with a.) Lansmont Model 23 Drop table, b.) Anatech event detector and c.) Keysight Data logger

For solder failure detection an Analysis Tech Model 32-106 was employed with the failure resistance threshold set to 150 Ohm and the event duration set to 1 µs while using a 10mA current supply. A Keysight 34980A data logger was also used for voltage monitoring of the 80-joint loop voltage and individual corner joint voltages. Sample failure was defined as the drop count in which an initial resistance disruption was identified by the event detector that was followed by the occurrence of three similar events in subsequent drops.

Two different table input acceleration G-levels were utilized in this study in order to evaluate how aging at room temperature affected both alloys. Specifically, a G-level of 340 was used for SAC305, while a G-level of 200 was chosen for the L29 alloy. These levels were decided upon based on setup samples which indicated that the SAC305 alloy could survive many times more drops than the L29 alloy under similar test conditions. Thus, it must be stressed that the SAC305 and L29 results are not being directly compared, but instead their trend behavior over time is being evaluated with the understanding that the L29 alloy is not expected to be as mechanically robust as the SAC305 alloy. (For reference: three L29 samples subjected to 340-G failed at drop numbers 1, 3, and 3).

Test Matrix:

The solder alloys used in this experiment were SAC305 and L29. All samples were stored at room temperature (approximately 23°C) in a controlled environment to ensure uniform starting conditions with stable temperature and humidity to minimize external influences on the samples. Shortly after the reflow process subset populations of each alloy were subjected to drop tests conducted within 60 minutes of exiting the oven.

SAC305 samples were subjected to aging at room temperature for specific durations: 3, 15, 30, and 50 days and then drop tests were conducted on the respective populations. In the case of the L29 alloy, aside from the samples subjected to drop tests shortly after reflow, samples were aged for up to 50 days with no predefined interval testing. Instead, samples were tested based on equipment availability. Table 1 provides the test schedules and sample sizes for the SAC305 and L29 populations.

Table 1. Test Matrix

Aging Time (days)	Sample Size	
	SAC305	L29
After Reflow	9	9
1	0	3
2	0	3
3	8	0
4	0	3
7	0	3
11	0	3
15	8	0
16	0	3
17	0	2
21	0	4
30	8	2
31	0	1
40	0	1
42	0	3
48	0	1
50	8	3

RESULTS

Drop Test

The test results reveal crucial insights into how aging impacts the shock resistance for both SAC305 and L29 solder alloys.

SAC305 samples subjected to drop testing at 340-G input shocks failed between 12 and 282 drops. Figure 4 provides a scatter plot of the SAC305 drop test data. The scatter plot indicates a slight trend of increasing reliability with time, but the effect appears to be small given the large variability in drop test performance from part to part. In fact, two sample T-tests comparing the means of the populations indicates that there is no significant difference between the sample sets at 95% confidence. Thus, it was concluded that up to 50 days after reflow at room temperature had little effect on SAC305 BGA performance for the drop test condition utilized.

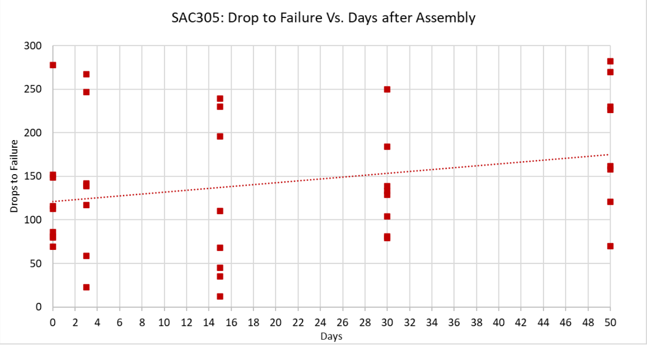

Figure 4. Scatter plot showing SAC305 drop data (340-G input)

Now, as shown in Figure 5, the L29 samples subjected to 200-G input shocks failed between 24 and 582 drops while demonstrating a measurable increase in shock survivability as aging time increased. For example, L29 samples subjected to drop testing within 60 minutes or less of reflow soldering failed in an average of 56 drops while those subjected to 40 or more days of aging survived an average of 316 drops, or a 5.6X increase in average life.

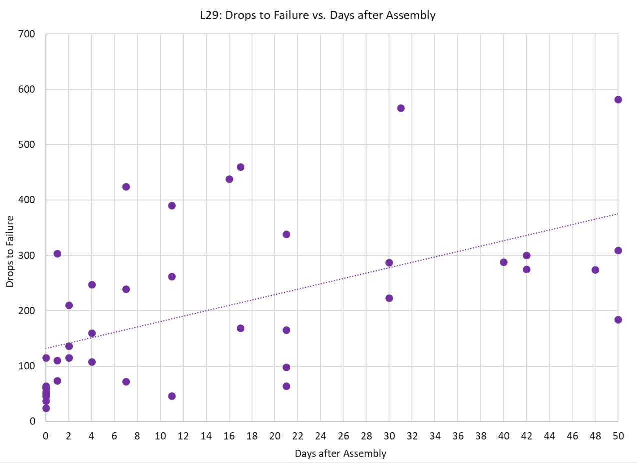

Figure 5. Scatter plot showing L29 drop data (200-G input)

The L29 populations were separated into five groups in order to produce 2-parameter Weibull plots due to the small sample sizes at each test interval. These Weibull plots are found in Figure 6. Examination of the plots shows that the least reliable condition was the After Reflow population which produced a characteristic lifetime of 63 drops. In comparison, the 1 to 4 day aging population produced a characteristic lifetime that was 3X greater than the After Reflow group (i.e. 181 drops) while the 7 to 17 day, 21 to 30 day and 40 to 50 day populations show 4.5 to 5.5X improvement over the After Reflow results.

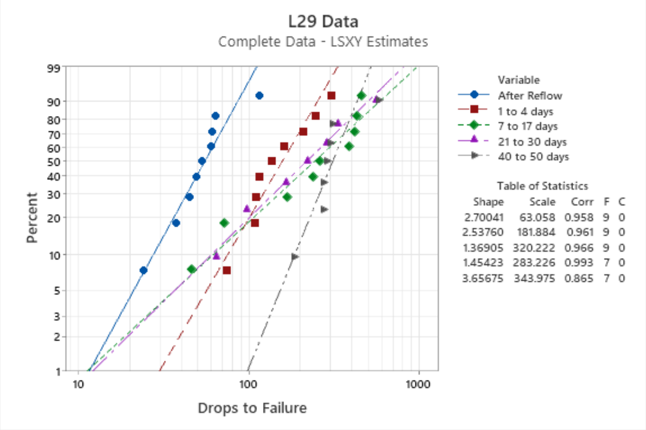

Table of Statistics

Shape	Scale	Corr	F	C
2.70041	63.058	0.958	9	0
2.53760	181.884	0.961	9	0
1.36905	320.222	0.966	9	0
1.45423	283.226	0.993	7	0
3.65675	343.975	0.865	7	0

Figure 6. Weibull plots showing L29 drop data (200-G input)

Much like the SAC305 populations, the L29 populations show significant part to part variability in terms of drop performance. In this case, the 7 to 17 and 21 to 30 day L29 populations each have two failures that occurred slightly early in test and which result in low Shape factors on the Weibull plots. It is likely that these early failures are typical for drop testing the L29 alloy and may occur somewhat randomly due to individual solder joint formation characteristics that can negatively impact reliability or from drop test variability (i.e. industry standard JESD22.B110B.01 allows +/-10% tolerance for shock test acceleration pulse). If these early failures are excluded from the analysis, the Weibull plots would strongly support the notion that L29 solder joint durability significantly increases over the first seven or so days following reflow.

Failure Mode Analysis

A detailed analysis of failure modes was undertaken on the SAC305 and L29 populations. Failure locations were identified during the drop test by using the datalogger information. All electrical failures were isolated to corner solder joint positions as was expected given the physical configuration of the drop test setup. Select samples were cross-sectioned and examined using optical and scanning electron microscopy.

SAC305 samples examined during the cross-sectional evaluation showed that multiple failure modes occurred during drop testing. Fortunately, all failure modes were associated with some form of solder joint damage and non-solder failure mechanisms such as pad cratering and trace cracking were not present in any of the samples.

As shown in Figure 7, one SAC305 failure mode was crack growth through and around the component side IMC. This failure mode was observed in only a few samples and was characterized by fine crack growth between the IMC and nickel layer and between the IMC and bulk solder with some degree of IMC cracking also occurring.

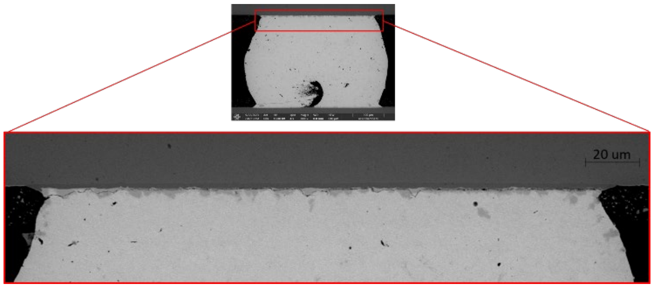

Figure 7. SAC305 solder joint from the After Reflow population. A fine crack has propagated through the IMC layer, between the IMC and bulk solder and between the IMC and nickel layer located near the component side pad.

Another failure mode observed in the SAC305 samples was a complete separation of the component side IMC from the BGA pad nickel layer. As shown in Figure 8, this failure mode was quite obvious in cross-section and is likely a brittle-type failure.

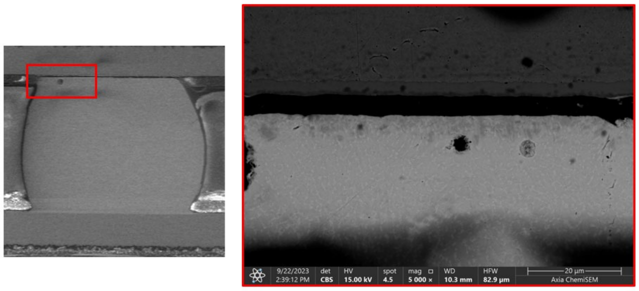

Figure 8. SAC305 solder joint from the 15 day population showing IMC to nickel layer failure.

An example of the most common SAC305 failure mode observed in cross-section is found in Figure 9. In this instance, it appears that the CuSn intermetallic has separated from the test board pad.

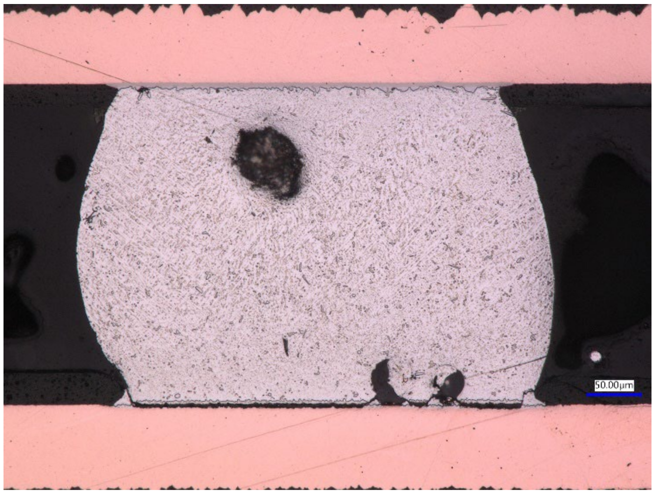

Figure 9. SAC305 solder joint from the After Reflow population showing IMC to PCB copper pad failure.

In the case of the SAC305 populations, there was no dominant failure mode for any given aging duration. Instead, most samples showed the IMC to BGA nickel separation and/or the IMC to PCB pad separation. Furthermore, no correlation between the number of drops to failure and the failure mode were identified.

Much like the SAC305 populations, cross-sectional evaluation of the L29 populations revealed multiple solder joint failure modes, with some joints containing more than one potential failure mode. Also, like the SAC305 populations, no non-solder failure modes were observed.

The most common L29 failure mode for the After Reflow population appeared to be a separation of the IMC from the BGA nickel layer as shown in Figures 10 and 11. This failure mode is presumably a brittle-type failure and explains why the After Reflow L29 population produced poor drop test results. This failure mode would also be observed among the aged populations (see Figure 12), but was not as common. However, when this failure mode occurred in the aged specimens, it was typically associated with earlier failures.

Figure 10. L29 solder joint from the After Reflow population. This joint failed at drop #46. There appears to be a clean separation between the BGA nickel layer and the IMC.

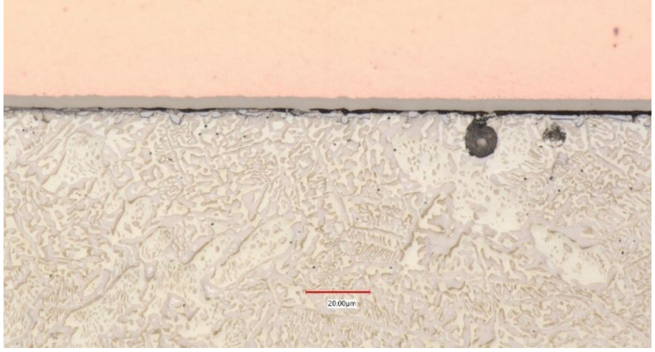

Figure 11. An enlarged view of an L29 solder joint from the After Reflow population. This joint failed at drop #51. There appears to be a clean separation between the BGA nickel layer and the IMC.

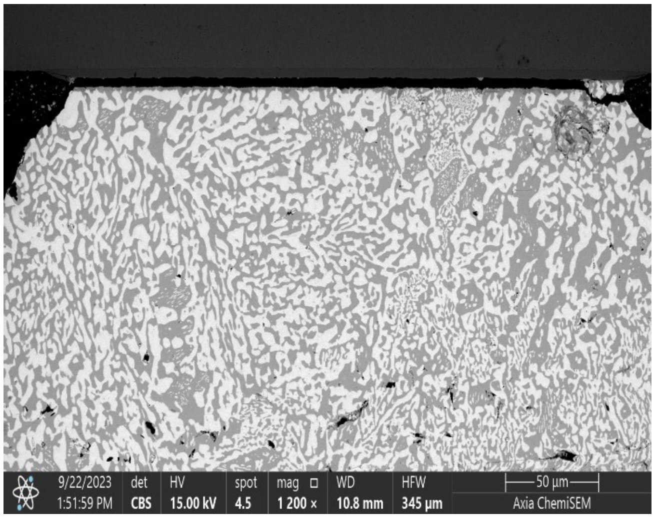

Figure 12. An L29 solder joint from the 17 day population. This joint failed at drop #169. There appears to be a clean separation between the BGA nickel layer and the IMC.

Bulk solder fatigue cracks were observed in many L29 samples and it was found that such fatigue could occur near either attachment pad as shown in Figure 13 and Figure 14. The fact that bulk solder fatigue could occur on either side of the solder joints was likely due to the fact that both sides of the joints were SMD with similarly sized mask openings. Overall, it appeared that bulk solder fatigue was more commonly found on the PCB side of the solder joint, which makes sense given that stresses from drop testing are generated through the flexing of the PCB. There was some evidence suggesting bulk solder fatigue was more common in longer aged samples -indicating that increasing time after reflow may have improved the IMC-to-pad robustness which ultimately shifted the failure from the IMC region and into the bulk solder.

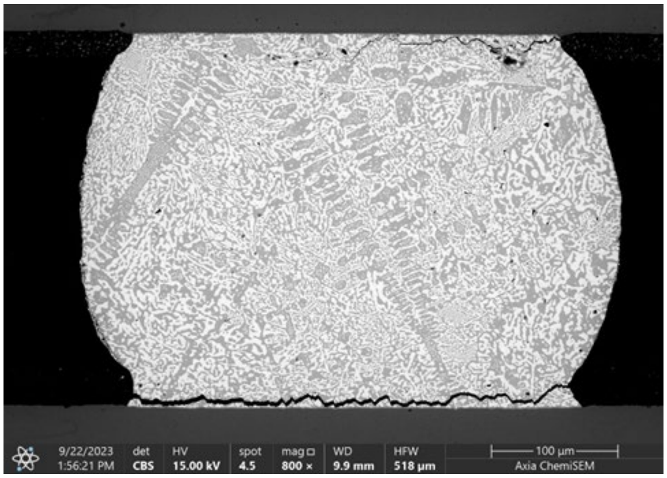

Figure 13. L29 solder joint from the 30 day population showing complete bulk solder failure near the PCB pad and partial bulk solder failure near the component side.

Figure 14. L29 solder joint from the 50 day population. This joint failed at drop #311. Crack growth occurred through the bulk solder above the PCB side IMC region.

CONCLUSIONS

This research investigated the impact of room-condition aging up through 50 days on SAC305 and L29 solder alloys using drop/shock testing as a means to evaluate solder joint reliability.

The study found that L29 solder joints were inherently more brittle than SAC305 solder joint owing to their bismuth content. This increased brittleness necessitated testing the L29 solder joints at a lower shock input pulse than the SAC305 solder joints. Due to the different test conditions, the experimental results for SAC305 and L29 are not meant to be directly compared, but instead the SAC305 results should be used to establish normal expectations for solder behavior over time.

It was found that SAC305 performance was not impacted by room-temperature aging with samples tested shortly after reflow soldering performing similarly to those tested 50 days later. Normal variability from part to part and within the drop test procedure were likely larger factors affecting the test results than the time after reflow.

Notably, the L29 alloy exhibited an improved drop/shock performance due to aging with samples tested shortly after reflow demonstrating 33 to 80% lower lifetime when compared to the various aged samples. These results indicate that the L29 samples are quite weak coming out of reflow and require perhaps 7 days or longer to mechanically stabilize.

Failure analysis revealed damage modes typically encountered during drop testing. In both cases, for SAC305 and L29, IMC to nickel layer failures were frequently observed at the corner solder joint positions. The IMC to nickel layer failures were associated with earlier failures for any given aging condition, and were found to be most common with the After Reflow test condition for the L29 solder.

Most failures were observed to occur near the PCB pad side of the joint. Both SAC305 and L29 samples produced failure due to separation between the copper PCB pads and IMC formation but only L29 was observed to result in bulk solder failure near the PCB pad. L29 Bulk solder failure was more likely to occur with aging indicating that the intermetallic strength of the L29 alloy was improving with time.

Cracking through and around the IMC layers was also encountered with SAC305 and L29, but to a lesser extent than the other modes.

REFERENCES

[1] 1. N. Jiang, L. Zhang, L.-L. Gao, X.-G. Song, and P. He, “Recent advances on SnBi low-temperature solder for electronic interconnections,” *Journal of Materials Science: Materials in Electronics*, vol. 32, no. 18, pp. 22731–22759, 2021.

[2] M. Ribas *et al.*, “Development of low-temperature drop shock resistant solder alloys for handheld devices,” in *2013 IEEE 15th Electronics Packaging Technology Conference (EPTC 2013)*, IEEE, 2013, pp. 48–52.

[3] M. Jian, A. Alahmer, X. Wei, M. E. A. Belhadi, A. Alakayleh, and S. Tahat, “Shear fatigue analysis of SAC-Bi solder joint exposed to varying stress cycling conditions,” *IEEE Trans Compon Packaging Manuf Technol*, vol. 13, no. 2, pp. 274–283, 2023.

[4] H. Zhang, S. Lytwynec, H. Wang, J. Geng, F. Mutuku, and N.-C. Lee, “An Alternative Lead-Free Low-Temperature Solder with Excellent Drop Shock Resistance,” in *Proceedings of SMTA International*, 2020, pp. 280–290.

[5] V. Jayaram, O. Gupte, K. Bhangaonkar, and C. Nair, “A Review of Low Temperature Solders in Microelectronics Packaging,” *IEEE Trans Compon Packaging Manuf Technol*, 2023.

[6] M. Ribas, T. Hunsinger, T. Cucu, H. V Ramakrishna, G. Lim, and M. Murphy, “The printed circuit assembler’s guide to low-temperature soldering,” *BR Publishing California*, 2018.

[7] K. N. Subramanian and D. R. Frear, “Issues related to the implementation of Pb-free electronic solders in consumer electronics,” *Lead-Free Electronic Solders: A Special Issue of the Journal of Materials Science: Materials in Electronics*, pp. 319–330, 2007.

[8] S. Mokler *et al.*, “The application of Bi-based solders for low temperature reflow to reduce cost while improving SMT yields in client computing systems,” in *Proceedings of SMTA International*, 2016, pp. 318–326.

[9] P. Liu, P. Yao, and J. Liu, “Effects of multiple reflows on interfacial reaction and shear strength of SnAgCu and SnPb solder joints with different PCB surface finishes,” *J Alloys Compd*, vol. 470, no. 1, pp.188–194,2009,doi: https://doi.org/10.1016/j.jallcom.2008.02.102.

[10] M. Maalekian, Y. Xu, and K. Seelig, “Efect of Bi content on properties of low silver SAC solder,” in *AIM Metals & Alloys Montreal*, Rosemont IL, Sept. 27–Oct. 1, 2015.

[11] M. E. A. Belhadi and A. Alahmer, “Effect of Bi content and aging on solder joint shear properties considering strain rate,” *Microelectronics Reliability*, vol. 146, p. 115020, 2023.

[12] L. Gao *et al.*, “Effect of alloying elements on properties and microstructures of SnAgCu solders,” *Microelectron Eng*, vol. 87, no. 11, pp. 2025–2034, 2010.

[13] J. Zhao, Y. Mutoh, Y. Miyashita, and S. L. Mannan, “Fatigue crack-growth behavior of Sn-Ag-Cu and Sn-Ag-Cu-Bi lead-free solders,” *J Electron Mater*, vol. 31, pp. 879–886, 2002.

[14] M. E. A. Belhadi, L. Wentlent, R. Al Athamneh, and S. Hamasha, “Mechanical Properties of SAC-Bi Solder Alloys with Aging,” in *Proceedings of 2019 SMTA International*, 2019, pp. 22–26.

[15] C.-M. Chuang, T.-S. Lui, and L.-H. Chen, “Effect of aluminum addition on tensile properties of naturally aged Sn-9Zn eutectic solder,” *J Mater Sci*, vol. 37, pp. 191–195, 2002.

[16] D. B. Hani, R. Al Athamneh, M. Aljarrah, and S. Hamasha, “Shear strength degradation modeling of lead-free solder joints at different isothermal aging conditions,” *Journal of Microelectronics and Electronic Packaging*, vol. 18, no. 3, pp. 137–144, 2021.

[17] Y.-S. Kim, K.-S. Kim, C.-W. Hwang, and K. Suganuma, “Effect of composition and cooling rate on microstructure and tensile properties of Sn–Zn–Bi alloys,” *J Alloys Compd*, vol. 352, no. 1–2, pp. 237–245, 2003.

[18] H. Ma, T.-K. Lee, D. H. Kim, S. H. Kim, H. G. Park, and K.-C. Liu, “Isothermal aging effects on the dynamic performance of lead-free solder joints,” in *2009 59th Electronic Components and Technology Conference*, IEEE, 2009, pp. 390–397.